Organometallics **1982**, *1*, 1211–1216 1211

82336-28-5; **5b**, 82293-81-0; **5c**, 82293-83-2; **5d**, 82322-76-7; **5e**, 82293-85-4; **5f**, 82293-87-6; **6**, 82293-88-7; (+)-(S_{Re})-**7**, 82293-90-1; (−)-(R_{Re})-**7**, 82336-30-9; (−)-(*RR*)-**8**, 82293-91-2; (+)-(*SR*)-**8**, 82372-77-8; (*SS*)-^{8}, 82336-31-0; (−)-(*R*)-**9**, 82336-32-1; (+)-(*S*)-**9**, 82336-33-2; (−)-(*R*)-^{1}0, 82336-34-3; (+)-(*S*)-**10**, 82336-35-4; (−)-(*R*)-**11**, 82336-36-5; (+)-(*S*)-**11**, 82336-37-6; (−)-(*S*)-α-(1-naphthyl)ethylamine, 10420-89-0; (+)-(*R*)-α-(1-naphthyl)ethylamine, 3886-70-2; $Ph_3C^+PF_6^-$, 437-17-2; (−)-Ph_2P(O-*l*-menthyl), 67392-57-8.

Supplementary Material Available: Figure 8, numbering of atoms in (−)-(*R*)-(η-C_5H_5)Re(NO)(PPh_3)($CH_2C_6H_5$) ((−)-(*R*)-**9**), Figure 9, crystal packing diagram of (−)-(*R*)-**9** as viewed down axis *a*, Figure 10, crystal packing diagram of (−)-(*R*)-**9** as viewed down axis *b*, Table III, summary of crystallographic data for (−)-(*R*)-**9**, Table IV, bond lengths and short interatomic nonbonded contacts in (−)-(*R*)-**9**, Table V, bond angles in (−)-(*R*)-**9**, Table VI, calculated atomic coordinates and thermal factors of (−)-(*R*)-**9**, Table VII, atomic coordinates of (−)-(*R*)-**9** (atoms refined anisotropically), and Table VIII, calculated and observed structure factors for (−)-(*R*)-9 (29 pages) Ordering information is given on any current masthead page.

Oxidative Addition of Halogens to Thiolato-Bridged Dinuclear Iridium(I) Complexes. Preparation of Several Iridium(II) and Iridium(III) Species. X-ray Structure of $Ir_2(\mu\text{-}t\text{-}BuS)_2(CO)_2(PMe_2Ph)_2I_2$[1]

Philippe Kalck*[2] and Jean-Jacques Bonnet

Laboratoire de Chimie de Coordiation du CNRS Associé à l'Université Paul Sabatier, 31400 Toulouse, France

Received March 26, 1982

Several oxidative reactions of different halogens to dinuclear complexes $Ir_2(\mu\text{-}t\text{-}BuS)_2(CO)_2L_2$ (L = CO, $P(OMe)_3$, PMe_2Ph, PMe_3) have been carried out in nondonor solvents such as toluene or dichloromethane. Different behavior has been observed depending upon the nature of the halogen. Addition of 1 molar equiv of iodine leads to quantitative formation of Ir(II) complexes of general formula $Ir_2(\mu\text{-}t\text{-}BuS)_2(CO)_2L_2I_2$. Further addition of a second molar equivalent of iodine gives rise to dinuclear iridium(III) compounds $Ir_2(\mu\text{-}t\text{-}BuS)_2(CO)_2L_2I_4$. Isomorphous complexes have been formed by addition of bromine. However, Ir(II) species could never be prepared quantitatively since Ir(III) complexes are always formed preferentially. Oxidative addition of chlorine has also been observed. However, substitution of both thiolato groups by chlorine atoms to give Ir(III) dinuclear complexes, $Ir_2(\mu\text{-}Cl)_2(CO)_2L_2Cl_4$, is a competitive process. An X-ray diffraction study of $Ir_2(\mu\text{-}t\text{-}BuS)_2(CO)_2(PMe_2Ph)_2I_2$ has been performed. This compound crystallizes with four formula units in the monoclinic space group C_{2h}^5—$P2_1/c$ in a cell of dimensions a = 16.997 (2) Å, b = 14.911 (3) Å, c = 13.411 (3) Å, and β = 91.17 (1)°. On the basis of 3390 unique reflections the structure was refined by full-matrix least-squares techniques to conventional indices $R(F)$ = 0.046 and $R_w(F)$ = 0.055. The molecular architecture of this dinuclear complex can be described in terms of two square-planar pyramids around each iridium atom sharing an edge formed by the two sulfur atoms. The flap angle between the two basal planes is 83.8°. The two iodine atoms occupy the two axial positions, and the two phosphine ligands are mutually cis; the Ir–Ir separation is of 2.702 (1) Å. Other bond distances of interest are the following: Ir (1)–I(1) = 2.742 (2) Å, Ir(2)–I(2) = 2.712 (2) Å, Ir(1)–P(1) = 2.318 (5) Å, Ir(2)–P(2) = 2.311 (5) Å, Ir (1)–S(1) = 2.383 (5) Å, Ir(1)–S(2) = 2.373 (5) Å, Ir(2)–S(1) = 2.372 (5) Å, Ir(2)–S(2) = 2.391 (5) Å.

Introduction

During our investigations of the reactivity of dinuclear iridium(I) complexes toward alkyl halides we observed the very fast reaction of 1 molar equiv of CH_3I to give appreciable amounts of complexes $Ir_2(\mu\text{-}t\text{-}BuS)_2(CO)_2(PR_3)_2I_2$. Such compounds, formulated as iridium(II) species, were of interest to us, and a systematic study of their preparation by direct oxidative addition of iodine was undertaken. An extension of such reactions to the other halogens has been carried out. Such complexes are, in principle, starting materials for the preparation of other such complexes by substitution of the iodide ligands. Moreover, there are very few known dinuclear iridium(II) complexes,[3–10] and since some of them were proposed as intermediates during the oxidative addition of alkyl halides to mononuclear iridium(I) complexes, the relevance to the mechanism of the addition prompted us to study the addition of iodine in more detail.

Experimental Section

Synthetic Work and Spectroscopic Data. The complexes $Ir_2(\mu\text{-}t\text{-}BuS)_2(CO)_4$ (**1**) and $Ir_2(\mu\text{-}t\text{-}BuS)_2(CO)_2L_2$ where L = P-

---

(1) Preliminary communication: Bonnet, J.-J.; Kalck, Ph.; Poilblanc, R. *Angew. Chem., Int. Ed. Engl.* **1980**, *19*, 551.

(2) To whom correspondence should be addressed at Laboratoire de Chimie Minérale et de Cristallochimie, Ecole Nationale Superieure de Chimie, 118 route de Narbonne, 31077 Toulouse Cedex, France.

(3) Moers, F. G.; de Jong, J. A. N.; Beaumont, P. M. H. *J. Inorg. Nucl. Chem.* **1973**, *35*, 1915.

(4) Angoletta, M.; Bellon, P. L.; Manassero, M.; Sansoni, M. *J. Organomet. Chem.* **1974**, *81*, C40.

(5) Mason, R.; Thomas, K. M.; Empsall, H. D.; Fletcher, S. R.; Heys, P. N.; Hyde, E. M.; Jones, C. E.; Shaw, B. L. *J. Chem. Soc., Chem. Commun.* **1974**, 612.

(6) Aranes, A.; Morazzoni, F.; Napoletano, T. *J. Chem. Soc.*, Dalton *Trans.* **1975**, 2039.

(7) Pilloni, G.; Schiavon, G.; Zotti, G.; Zecchin, S. *J. Organomet. Chem.* **1977**, *134*, 305.

(8) Angoletta, M.; Malatesta, L.; Caglio, G. *J. Chem. Soc.*, Dalton *Trans.* **1977**, 2131.

(9) Bonnet, J.-J.; Thorez, A.; Maisonnat, A.; Galy, J.; Poilblanc, R. *J. Am. Chem. Soc.* **1979**, *101*, 5940.

(10) Kalck, Ph.; Bonnet, J.-J.; Poilblanc, R. *J. Am. Chem. Soc.* **1982**, *104*, 3069.

0276-7333/82/2301-1211$01.25/0 © 1982 American Chemical Society

$(OMe)_3$ (**2**), PMe_2Ph (**3**), and PMe_3 (**4**) were prepared as previously described.[11,12] Since the starting materials are air sensitive, all reactions were carried out under dry oxygen-free nitrogen by using solvents saturated with nitrogen prior to use. Hexachloroiridic acid, *tert*-butyl mercaptan, *n*-butyllithium, trimethyl phosphite, iodine, bromine, chlorine, iodine monobromide, and galvinoxyl were of commercial origin.

Infrared spectra were obtained with a Perkin-Elmer 225 grating apparatus equipped with a scale expander working in optical density. Either hexadecane, dichloromethane solutions, or cesium bromide pellets were the media used. In the ν_{CO} region of interest, the spectra were calibrated by water vapor lines. ^1H and ^{31}P NMR spectra were obtained on a Bruker WH 90 spectrometer and ^{13}C spectra on a Cameca apparatus (62.86 MHz). Deuteriochloroform was used as solvent and tetramethylsilane as internal standard.

Elemental analyses were carried out by the "Service Central de microanalyses du C.N.R.S.". Molecular weights were determined by tonometry in benzene solutions by using a Mechrolab apparatus.

Preparation of $Ir_2(\mu$-*t*-$BuS)_2(CO)_2L_2I_2$, 5 (L = CO). A 0.1836-g sample of $Ir_2(\mu$-*t*-$BuS)_2(CO)_4$ (0.27 mmol) was dissolved in 10 mL of CH_2Cl_2, and 0.069 g of iodine (0.27 mmol) was added at -10 °C with stirring. The originally yellow solution turned red. After completion of the reaction (monitored by IR) the solvent was evaporated slowly under reduced pressure. A bright red powder was obtained: 0.245 g (97%); IR (hexadecane) anti isomer,[13] 2099 (vs.), 2078 (m), 2046 (vs) cm^{-1} (ν_{CO}); syn-endo isomer, 2092 (vs), 2069 (m), 2039 (vs) cm^{-1} (ν_{CO}), (CsBr) 2096 (vs), 2074 (s), 2053 (s), 2045 (s), 2037 (s) cm^{-1}; ^1H NMR ($CDCl_3$) 1.58, 1.64, 1.65 ppm (*t*-BuS); ^{13}C NMR anti isomer, 164.09, 162.30 (CO), 60.76 (Me_3*C* exo), 52.23 (Me_3*C* endo), 34.78 (*Me*$_3$C exo), 33.78 (*Me*$_3$C endo), syn-endo isomer 165.48 (CO), 54.29 (Me_3*C*), 33.78 ppm (*Me*$_3$C). Anal. Calcd for $C_{12}H_{18}O_4S_2I_2Ir_2$: C, 15.52; H, 1.95; S, 6.91; I, 27.33. Found: C, 15.72; H, 2.07; S, 6.79; I, 27.13 (mol wt calcd 929, found 938).

6 (L = $P(OCH_3)_3$). A 0.3671-g sample of $Ir_2(\mu$-*t*-$BuS)_2(CO)_2(P(OMe)_3)_2$ (0.42 mmol) was dissolved in 20 mL of toluene, and 0.1075 g of iodine (0.42 mmol) was added at room temperature. The orange solution turned red, and after complete dissolution of I_2 the infrared spectra revealed the absence of any starting material. Stirring was continued for 30 min. The solution was concentrated under reduced pressure to about 10 mL, and hexane was added in two layers. Crystallization at -25 °C gave 0.450 g of red crystals (85%): mp 162 °C dec; IR (CH_2Cl_2) cis-anti isomer, 2025 (vs), 2005 (m) cm^{-1} (ν_{CO}), (CsBr) 2014 (vs) 1986 (m) cm^{-1} (ν_{CO}); ^1H NMR ($CDCl_3$) 1.57 (*t*-BuS endo), 1.63 (t, J_{PH} = 0.7 Hz, *t*-BuS exo), 3.85 ppm (d, J_{PH} = 11.3 Hz, $P(OMe)_3$); $^{31}P\{^1H\}$ NMR ($CDCl_3$) 79.1 ppm; ^{13}C NMR ($CDCl_3$) 170.40 (d, J_{PC} = 14.8 Hz, CO), 54.40 ($P(OCH_3)_3$), 34.72 (C(*CH*$_3$)$_3$ exo), 33.95 (C-(*CH*$_3$)$_3$ endo), 57.18 (C(*CH*$_3$)$_3$ exo), 50.34 ppm (*C*-(CH$_3$)$_3$ endo). Anal. Calcd for $C_{16}H_{36}O_8P_2S_2I_2Ir_2$: C, 17.15; H, 3.24; S, 5.72; I, 22.65. Found: C, 17.26; H, 3.15; S, 5.60; I, 22.4.

7 (L = PMe_2Ph). As the complex Ir_2 (μ-*t*-$BuS)_2(CO)_2(PMe_2Ph)_2$ cannot be obtained in the solid form, it was prepared by direct addition of 0.077 mL of PMe_2Ph (0.54 mmol) to 0.1814 g (0.27 mmol) of **1** in 15 mL of toluene. Agitation was maintained for 15 min, and decarbonylation, as shown by the IR spectra, was achieved under a slightly reduced pressure. Then 0.068 g of iodine (0.27 mmol) was added, giving a red solution. After 1 h, hexane was added in two layers. By slow mutual diffusion of the two solvents at -25 °C crystallization occurred. Red crystals, 0.278 g, were obtained (90%): mp 222 °C; IR (CH_2Cl_2) cis-anti isomer, 2007 (vs), 1990 (m sh) cm^{-1} (ν_{CO}), (CsBr) 1998 (vs), 1981 (m) cm^{-1} (ν_{CO}); ^1H NMR ($CDCl_3$) 1.42 (*t*-BuS endo), 1.62 (*t*-BuS exo), 2.17, 1.78 ppm (J_{PH} = 10.7 Hz, $P(CH_3)_2$). Anal. Calcd for $C_{26}H_{40}O_2S_2P_2I_2Ir_2$: C, 27.18; H, 3.51; S, 5.58; I, 22.09. Found: C, 27.08; H, 3.54; S, 5.43; I, 21.94.

8 (L = PMe_3). A 0.4190-g sample of $Ir_2(\mu$-*t*-$BuS)_2(CO)_2(PMe_3)_2$ (0.54 mmol) was dissolved in 20 mL of toluene, and 0.1379 g of iodine (0.54 mmol) was added at room temperature. The solution was stirred for 1 h. Petroleum ether (bp 35–45 °C fraction) was added in order to have two layers. Crystallization at -25 °C gave 0.512 g of twinned brick-red crystals (92%), mp 202 °C. Anal. Calcd for $C_{16}H_{36}O_2P_2S_2I_2Ir_2$: C, 18.75; H, 3.54; S, 6.26; I, 24.77. Found: C, 19.15; H, 3.56; S, 5.98; I, 23.95. Recrystallization in toluene/hexane gave first red crystals which were identified as the cis-anti isomer: mp 206 °C; IR (CH_2Cl_2) 2004 (vs), 1982 (m) cm^{-1} (ν_{CO}), (CsBr) 1995 (vs), 1970 (m) cm^{-1} (ν_{CO}); ^1H NMR ($CDCl_3$) 1.52 (*t*-BuS endo), 1.65 (*t*-BuS exo), 2.06 (d, J_{PH} = 11.0 Hz, $P(CH_3)_3$); $^{31}P\{^1H\}$ NMR ($CDCl_3$) -44.1 ppm; $^{13}C\{^1H\}$ NMR ($CDCl_3$) 172.29 (d, J_{PC} = 13.0 Hz, CO), 56.70 (S*C*Me$_3$ exo), 49.30 (S*C*Me$_3$ endo), 33.93 (SC(*CH*$_3$)$_3$ exo), 33.28 (SC(*CH*$_3$)$_3$ endo), 20.04 ppm (d, J_{PC} = 40.8 Hz, $P(CH_3)_3$). At the end of the crystallization orange-red twinned crystals were obtained which were identified as the trans-anti isomer: mp 204 °C; IR (CH_2Cl_2) 2011 (vs), 1980 (m) cm^{-1} (ν_{CO}), (CsBr) 2008 (vs), 1977 (m) cm^{-1} (ν_{CO}); ^1H NMR ($CDCl_3$) 1.52 and 1.56 (*t*-BuS endo and exo) 2.19 (d, J_{PH} = 10.8 Hz, $P(CH_3)_3$), 2.11 ppm (d, J_{PH} = 11.4, $P(CH_3)_3$); $^{31}P\{^1H\}$ NMR ($CDCl_3$) -37.1, -64.8 ppm ($P(CH_3)_3$); $^{13}C\{^1H\}$ NMR ($CDCl_3$) 172.18 (CO), 168.54 (CO), 57.55 (S*C*Me$_3$ exo), 52.99 (S*C*Me$_3$ endo), 34.04 (SC(*CH*$_3$)$_3$ exo), 32.81 (SC(*CH*$_3$)$_3$ endo), 21.89 (d, J_{PC} = 37.0 Hz, $P(CH_3)_3$), 20.27 ppm (d, J_{PC} = 40.7 Hz, $P(CH_3)_3$).

Preparation of $Ir_2(\mu$-*t*-$BuS)_2(CO)_2L_2X_4$, 9 (L = CO; X = Br). A 0.017-mL sample of bromine (0.334 mmol) was added to 10 mL of a solution containing 0.1126 g of $Ir_2(\mu$-*t*-$BuS)_2(CO)_4$ (0.167 mmol). The bright bronze color turned yellow. After 10 min a yellow precipitate appeared. The precipitation was completed by addition of pentane. The yellow powder was washed with pentane and dried under reduced pressure (0.146 g, 86%): mp 196 °C; IR (CH_2Cl_2) 2138 (vs), 2099 (s) cm^{-1} (ν_{CO}), (CsBr) 2135 (vs), 2093 (s) cm^{-1} (ν_{CO}); ^1H NMR ($CDCl_3$) 1.57 and 1.64 ppm (*t*-BuS). Anal. Calcd for $C_{12}H_{18}O_4S_2Br_4Ir_2$: C, 14.49; H, 1.82; S, 6.45; Br, 32.14. Found: C, 14.88; H, 1.87; S, 6.27; Br, 32.13.

10 (L = CO; X = I). A 0.247-g sample of $Ir_2(\mu$-*t*-$BuS)_2(CO)_4$ (0.184 mmol) was dissolved in 10 mL of toluene, and 0.0938 g of iodine (0.37 mmol) was added slowly. The red solution was stirred for 2 h. Addition of hexane and crystallization at -25 °C followed by washing with hexane and drying under reduced pressure gave microcrystals (0.185 g, 85%, mp 188 °C). Separation of isomers by recrystallization was unsuccessful. Similar results were obtained when 1 molar equiv of iodine was added to **5**: IR (CH_2Cl_2) 2127 (s), 2106 (vs), 2088 (s), 2084 (m sh) cm^{-1} (ν_{CO}); ^1H NMR ($CDCl_3$) 1.76, 1.61 ppm (*t*-BuS). Anal. Calcd for $C_{12}H_{18}O_4S_2I_4Ir_2$: C, 12.19; H, 1.53; S, 5.42; I, 42.93. Found: C, 12.52; H, 1.67; S, 5.12; I, 42.84.

11 (L = $P(OMe)_3$; X = Br). Similar to the preparation of complex **9**, complex **11** was obtained as a yellow powder (yield 90%; mp 153 °C) by addition at room temperature of 2 molar equiv of bromine to $Ir_2(\mu$-*t*-$BuS)_2(CO)_2(P(OMe)_3)_2$: IR (CH_2Cl_2) 2072 (vs br) cm^{-1} (ν_{CO}), (CsBr) 2064 (vs br) cm^{-1} (ν_{CO}); ^1H NMR ($CDCl_3$) 1.71, 1.68, 1.61, 1.58 (*t*-BuS), 3.97 (d, J_{PH} = 11.2 Hz, $P(OMe)_3$), 3.94 (d, J_{PH} = 11.2 Hz, $P(OMe)_3$), 3.69 (d, *J* = 11.2 Hz, $P(OMe)_3$), 3.63 ppm (d, J_{PH} = 11.2 Hz, $P(OMe)_3$). Anal. Calcd for $C_{16}H_{36}O_8P_2S_2Br_4Ir_2$: C, 16.19; H, 3.06; S, 5.40; Br, 26.94. Found: C, 16.34; H, 3.14; S, 5.59; Br, 26.66.

12 (L = $P(OMe)_3$; X = I). Addition of 1 molar equiv of iodine to complex **6** in toluene solution gave a quantitative yield of complex **12**. Crystallization was performed at -25 °C in toluene/hexane solution: IR (CH_2Cl_2) 2067 (vs br) cm^{-1} (ν_{CO}), (CsBr) 2063 (vs br) cm^{-1} (ν_{CO}); ^1H NMR ($CDCl_3$) 1.78, 1.66 (*t*-BuS), 3.99 (d, J_{PH} = 11.2 Hz, $P(OMe)_3$), 3.97 (d, J_{PH} = 11.2 Hz, $P(OMe)_3$), 3.72 (d, J_{PH} = 11.2 Hz, $P(OMe)_3$), 3.65 ppm (d, J_{PH} = 11.2 Hz,

---

(11) de Montauzon, D.; Poilblanc, R. *Inorg. Synth.* **1980**, *20*, 236.

(12) de Montauzon, D.; Kalck, Ph.; Poilblanc, R. *J. Organomet. Chem.* **1980**, *186*, 121.

(13) The figure shows the isomerism due to the relative position of the two CO ligands (cis or trans) and of the two *t*-Bu groups (in this case anti).

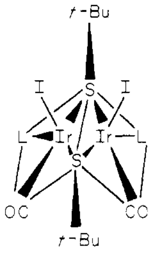

cis-anti isomer

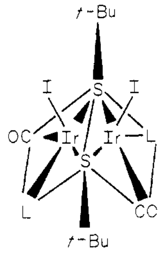

trans-anti isomer

Table II. Positional and Thermal Parameters for the Nongroup Atoms of $Ir_2(\mu\text{-}t\text{-BuS})_2(CO)_2(PMe_2Ph)_2I_2$ [a]

atom	x	y	z	β_{11}	β_{22}	β_{33}	β_{12}	β_{13}	β_{23}
Ir(1)	0.28715 (5)	0.05507 (5)	0.18771 (6)	2.37 (3)	1.85 (4)	3.56 (5)	0.01 (3)	−0.27 (3)	−0.11 (3)
Ir(2)	0.16427 (5)	−0.02421 (5)	0.27721 (6)	2.48 (3)	1.88 (4)	4.30 (5)	−0.10 (3)	−0.03 (3)	−0.02 (4)
I(1)	0.32454 (9)	0.17473 (10)	0.0409 (1)	5.04 (7)	3.98 (8)	4.58 (9)	−0.90 (6)	−0.29 (7)	1.18 (7)
I(2)	0.00601 (8)	−0.0160 (1)	0.2972 (1)	2.76 (6)	4.88 (9)	8.3 (1)	−0.60 (6)	0.24 (7)	−0.37 (8)
P(1)	0.3901 (3)	0.1025 (3)	0.2908 (4)	2.5 (2)	2.3 (2)	4.0 (3)	−0.1 (2)	−0.1 (2)	0.0 (2)
P(2)	0.1847 (3)	−0.0557 (4)	0.4445 (4)	4.0 (3)	2.8 (3)	4.2 (3)	0.3 (2)	0.5 (2)	0.3 (3)
S(1)	0.1640 (3)	0.0218 (3)	0.1079 (4)	3.0 (2)	2.2 (2)	4.0 (3)	0.1 (2)	−0.7 (2)	−0.3 (2)
S(2)	0.2019 (3)	0.1292 (3)	0.2988 (3)	2.5 (2)	1.9 (2)	4.0 (3)	0.2 (2)	−0.5 (2)	−0.2 (2)
C(1)	0.350 (1)	−0.031 (2)	0.144 (1)	3.2 (7)	4 (2)	3 (1)	−2 (1)	−1.3 (7)	0 (1)
C(2)	0.161 (1)	−0.148 (2)	0.254 (2)	8 (1)	2 (1)	5 (2)	0 (1)	0 (1)	−1 (1)
C(3)	0.158 (1)	−0.066 (1)	0.009 (1)	3.6 (9)	3 (1)	3 (1)	−0.3 (8)	−0.5 (8)	0.0 (9)
C(4)	0.077 (1)	−0.111 (1)	0.019 (2)	2.9 (9)	5 (1)	7 (2)	−0.3 (9)	−1.4 (10)	−1 (1)
C(5)	0.225 (1)	−0.133 (1)	0.009 (2)	3.8 (10)	4 (1)	5 (2)	0.8 (9)	−0.7 (10)	−2 (1)
C(6)	0.160 (1)	−0.011 (2)	−0.086 (2)	5 (1)	7 (2)	5 (1)	−2 (1)	−2 (1)	−1 (1)
C(7)	0.135 (1)	0.226 (1)	0.263 (1)	2.0 (8)	3 (1)	6 (1)	0.7 (7)	−1.8 (8)	−0.2 (10)
C(8)	0.194 (1)	0.307 (1)	0.253 (1)	5 (1)	2 (1)	5 (1)	0.1 (8)	−1.1 (10)	−0.7 (10)
C(9)	0.080 (1)	0.239 (1)	0.353 (2)	4 (1)	4 (1)	6 (2)	1.2 (9)	1 (1)	−1 (1)
C(10)	0.090 (1)	0.213 (1)	0.165 (2)	5 (1)	5 (1)	6 (2)	2 (1)	−2 (1)	−1 (1)
C(11)	0.412 (1)	0.222 (1)	0.283 (2)	4.1 (10)	0.9 (9)	9 (2)	0.2 (8)	−2 (1)	−1 (1)
C(12)	0.379 (1)	0.088 (1)	0.425 (1)	3.7 (9)	4 (1)	3 (1)	−0.6 (8)	1.4 (9)	−1.2 (10)
C(19)	0.112 (1)	−0.132 (1)	0.499 (2)	4 (1)	5 (1)	7 (2)	−1.7 (10)	1 (1)	0 (1)
C(20)	0.181 (1)	0.038 (1)	0.528 (1)	8 (1)	3 (1)	4 (1)	−1.0 (10)	1 (1)	−0.8 (10)
O(1)	0.3940 (9)	−0.094 (1)	0.125 (1)	3.2 (7)	6 (1)	13 (2)	1.1 (7)	−1.1 (9)	−5 (1)
O(2)	0.162 (1)	−0.222 (1)	0.245 (1)	10 (1)	2.8 (9)	8 (1)	−1.2 (8)	0 (1)	0.0 (9)

[a] Estimated standard deviations in the least significant figure(s) are given in parentheses in this and all subsequent tables. The form of the anisotropic thermal ellipsoid is $\exp[-(\beta_{11}h^2 + \beta_{22}k^2 + \beta_{33}l^2 + 2\beta_{12}hk + 2\beta_{13}hl + 2\beta_{23}kl)]$. The quantities given in the table are the thermal coefficients $\times 10^3$.

$P(OMe)_3$). Anal. Calcd for $C_{16}H_{36}O_8P_2S_2I_4Ir_2$: C, 13.98; H, 2.64; S, 4.66; I, 36.93. Found: C, 14.33; H, 2.68; S, 4.57; I, 36.98.

13 (L = PMe₃; X = I). The addition of 1 molar equiv of iodine to complex 8 was performed at −5 °C in CH_2Cl_2 solution. Addition of petroleum ether and crystallization at −25 °C gave a red wax. Recrystallization from toluene/petroleum ether solution gave a red powder (70%): mp 222 °C; IR (CH_2Cl_2) 2066 (vs br) cm^{-1} (ν_{CO}), (CsBr) 2059 (vs br) cm^{-1} (ν_{CO}); ^1H NMR ($CDCl_3$) 1.75, 1.71 (*t*-BuS), 2.20 (d, J_{PH} = 11.2 Hz, PMe_3), 1.76, 1.68, 1.65 (*t*-BuS), 2.22 (d, J_{PH} = 11.2 Hz, PMe_3), 1.94 (d, J_{PH} = 11.2 Hz, PMe_3), 2.00 (d, J_{PH} = 11.2 Hz, PMe_3), 1.96 ppm (d, J_{PH} = 11.2 Hz, PMe_3). Anal. Calcd for $C_{16}H_{36}O_2P_2S_2I_4Ir_2$: C, 15.03; H, 2.84; S, 5.02; I, 39.70. Found: C, 15.77; H, 2.99; S, 4.83; I, 39.52.

Preparation of $Ir_2(\mu\text{-}Cl)_2(CO)_2L_2Cl_4$, 14 (L = CO). A 0.1930-g sample of complex 1 was dissolved in 15 mL of dichloromethane, and chlorine was bubbled in the solution for 30 min. The bronze solution turned rapidly red and then yellow, and a pale yellow precipitate appeared. Precipitation was completed by addition of petroleum ether. The powder was washed and dried under reduced pressure (0.142 g, 70%): mp 230 °C; IR (CH_2Cl_2) 2158 (vs), 2127 (vs) cm^{-1} (ν_{CO}), (CsBr) 2148 (vs), 2121 (vs) cm^{-1} (ν_{CO}); Raman (KBr) 2220 (vs), 2210 (vs) cm^{-1} (ν_{CO}). Anal. Calcd for $C_4O_4Cl_6Ir_2$: C, 6.77; Cl, 29.99. Found: C, 6.54; H, traces; Cl, 29.57.

15 (L = P(OMe)₃). Similarly this complex was obtained by chlorination of $Ir_2(\mu\text{-}t\text{-BuS})_2(CO)_2(P(OMe)_3)_2$ at room temperature. The pale yellow powder obtained was analyzed as $Ir_2Cl_6(CO)_2(P(OMe)_3)_2$ (yield 92%), mp 205 °C. Anal. Calcd for $C_8H_{18}O_8Cl_6P_2Ir_2$: C, 10.66; H, 2.01; Cl, 23.60. Found: C, 10.62; H, 2.01; S, traces; Cl, 23.17.

Collection and Reduction of X-ray Data for Compound 7. Preliminary Laue and precession photographs indicated monoclinic symmetry. Systematic extinctions (0*k*0, *k* = 2*n* + 1, and *h*0*l*, *l* = 2*n* + 1) are consistent with space group C_{2h}^5—$P2_1/c$. The selected crystal was centered on a Nonius CAD-4 diffractometer. Unit-cell parameters were obtained from a least-squares fit of the setting angles of the Mo Kα peaks of 25 high-angle reflections. These parameters are reported in Table I together with pertinent crystal data. Intensities were collected by using the ω–2θ scan technique. The scan width was $(1 + 0.35 \tan \theta)°$. Background measurements were obtained during a scan, at each end of the scan interval, with the total duration equal to half of the scan time. A total of 5752 intensities ($h > 0$, $k > 0$, $\pm l$) were measured within the interval $3 < 2\theta(\text{Mo K}\alpha) < 48°$. Four check reflections were monitored every 2 h of X-ray exposure and showed no significant changes in intensity.

Data processing was carried out by using a local program.[14] Peak counts were corrected for background to yield the net integrated intensity *I*. The standard deviations of the intensities were calculated according to the formula $\sigma(I) = \{CT + 0.25(B_1 + B_2) + (pI)^2\}^{1/2}$, where CT is the total integrated peak count, B_1 and B_2 are background counts and $I = Ct - 0.5(B_1 + B_2)$. The value of *p* was selected as 0.02. The values of *I* and $\sigma(I)$ were next corrected for Lorentz and polarization effects. The 3390 unique reflections having $F_o^2 > 3\sigma(F_o^2)$ were used in subsequent calculations. An absorption correction was applied to the data.[14]

Solution and Refinement of the Structure. The structure was solved by standard Patterson and Fourier methods and refined by full-matrix least-squares techniques.[14] Values of the atomic scattering factors and the anomalous terms were from the usual sources.[15] The effects of anomalous dispersion for the Ir, S, and P atoms were included in F_c.[16] The phenyl rings attached to P atoms were treated as rigid groups (D_{6h} symmetry, C–C distance of 1.392 Å). Refinement of an isotropic model converged to $R(F) = 0.082$ and $R_w(F) = 0.092$.

Anisotropic thermal parameters were then used for the 24 independent atoms, while carbon atoms of the phenyl rings were assigned isotropic thermal parameters. The final agreement factors were $R(F) = 0.046$ and $R_w(F) = 0.055$. A final difference Fourier map shows some peaks of the order 0.5 (2) e/Å^3 associated with the benzene rings. These peaks are approximately 10% of the heights of typical light-atom peaks on earlier Fourier map. Thus the final difference Fourier map is essentially featureless.

In Table II we present the atomic parameters of the nongroup atoms together with their standard deviations as derived from the inverse matrix. Group parameters appear in Table III. Table IV lists the root-mean-square amplitudes of vibration for those atoms refined anisotropically.[17] A listing of F_o vs. F_c is available.[17]

---

(14) All calculations have been performed by using CII IRIS 80 computer of the "Centre Interuniversitaire de Calcul de Toulouse". In addition to various local programs, modified versions of the following ones were employed: Ibers' AGNOST absorption program which includes both the Coppens–Leisserrowitz–Rabinovich logic for Gaussian integration and the Tompa de Meulenaur analytical method; Zalkin's FORDAP Fourier summation program; Johnson's ORTEP thermal ellipsoid plotting program; Busing and Levy's ORFFE error function program; Ibers' NUCLS full-matrix least-squares program, which in its nongroup form resembles the Busing and Levy's ORFLS program.

(15) Cromer, D. T.; Waber, J. T. "International Tables for X-ray Crystallography"; Kynoch Press: Birmingham, England, 1974; Vol. IV, Table 2.2A. Cromer, D. T. *Ibid.* Table 2.3.1.

(16) Ibers, J. A.; Hamilton, W. C. *Acta Crystallogr.* **1964**, *17*, 781–782.

Table III. Derived Parameters for the Rigid-Group Atoms of $Ir_2(\mu\text{-}t\text{-}BuS)_2(CO)_2(PMe_2Ph)_2I_2$

atom	*x*	*y*	*z*	*B*, Å^2	atom	*x*	*y*	*z*	*B*, Å^2
C(13)	0.4840 (6)	0.0508 (9)	0.2645 (10)	3.1 (4)	C(21)	0.2779 (6)	−0.1164 (9)	0.473 (1)	2.9 (4)
C(14)	0.5202 (8)	0.0730 (9)	0.1756 (9)	4.0 (5)	C(22)	0.3246 (8)	−0.1469 (10)	0.3960 (7)	4.3 (5)
C(15)	0.5911 (8)	0.033 (1)	0.1511 (9)	6.3 (6)	C(23)	0.3921 (8)	−0.197 (1)	0.4176 (10)	5.2 (5)
C(16)	0.6259 (7)	−0.030 (1)	0.215 (1)	5.9 (6)	C(24)	0.4130 (7)	−0.2158 (10)	0.516 (1)	5.2 (5)
C(17)	0.5898 (8)	−0.0517 (9)	0.304 (1)	4.6 (5)	C(25)	0.3664 (9)	−0.185 (1)	0.5932 (8)	5.2 (5)
C(18)	0.5188 (8)	−0.0115 (9)	0.3288 (8)	3.7 (4)	C(26)	0.2988 (8)	−0.1356 (10)	0.5716 (8)	4.9 (5)

Rigid-Group Parameters[a]

group	x_C	y_C	z_C	Δ	ϵ	η
ϕ(1)	0.5550 (5)	0.0107 (6)	0.2399 (7)	−3.16 (2)	−2.121 (9)	0.51 (2)
ϕ(2)	0.3455 (5)	−0.1661 (6)	0.4946 (7)	1.20 (5)	−1.767 (8)	−1.37 (5)

[a] x_C, y_C, and z_C are the fractional coordinates of the origin of the rigid group. The rigid-group orientation angles Δ, ϵ, and η (radians) have been defined previously (La Placa, S. J.; Ibers, J. A. *Acta Crystallogr.* **1965**, *18*, 511).

Results and Discussion

Syntheses of Compounds 5–15. The syntheses of compounds 5–15 as described in the Experimental Section show the following trends in the chemistry of oxidative addition of halogens to thiolato-bridged dinuclear iridium(I) compounds. The more interesting reactions have been observed when oxidative reactions are carried out by the direct action of iodine. Indeed, even at room temperature, addition of 1 molar equiv of iodine/equiv of starting material gives compounds corresponding to the first step of the oxidative process, i.e., complexes of Ir(II) in quantitative yield. Reactions of these Ir(II) compounds with a second equivalent of iodine finally give Ir(III) complexes. Thus, reactions leading to compounds **5**–**8** can be written as shown in eq 1, where L = CO, P(OMe)$_3$,

$$Ir_2(\mu\text{-}t\text{-}BuS)_2(CO)_2L_2 + I_2 \xrightarrow[\text{toluene}]{20\ °C} Ir_2(\mu\text{-}t\text{-}BuS)_2(CO)_2L_2I_2 \quad (1)$$

PMe$_2$Ph, and PMe$_3$. Reactions giving compounds **10**, **12**, and **13** proceed as shown in eq 2.

$$Ir_2(\mu\text{-}t\text{-}BuS)_2(CO)_2L_2I_2 + I_2 \xrightarrow[\text{toluene}]{20\ °C} Ir_2(\mu\text{-}t\text{-}BuS)_2(CO)_2L_2I_4 \quad (2)$$

All these compounds are obtained in very clean reactions (easily effected, high yields, products isolated as pure crystalline materials). A slight excess of iodine, even in concentrated solutions of Ir(II) complexes, does not lead to dinuclear Ir(III) compounds other than those described in eq 2. For instance, no substitution of the thiolato-bridging groups by iodide has been observed. The ν_{CO} stretching frequencies are, as expected, ca. 50 cm^{-1} higher in Ir(II) complexes and ca. 100 cm^{-1} higher in Ir(III) dinuclear compounds than in the starting Ir(I) complexes (see Experimental Section).

The behavior of bromine is somewhat different than that of iodine. Indeed, although the general scheme presented by the above reactions 1 and 2 still describes the oxidative action of bromine, Ir(II) compounds of type $Ir_2(\mu\text{-}t\text{-}BuS)_2(CO)_2L_2Br_2$ cannot be obtained as pure materials because the second step leading to Ir(III) complexes takes place very quickly and gives rise to compounds $Ir_2(\mu\text{-}t\text{-}BuS)_2(CO)_2L_2Br_4$ (L = CO, **9**; L = P(OMe)$_3$, **11**). However, Ir(II) compounds with bromine substituents have been detected by IR spectroscopy during the slow addition of bromine to dilute solutions of the starting Ir(I) materials. Indeed, the IR spectra after addition of 1 equiv of bromine show ν_{CO} stretching frequencies ca. 100 and 50 cm^{-1} higher than those observed for the starting Ir(I) dinuclear complex. They are fully consistent with the simultaneous presence of Ir(III) and Ir(II) compounds, respectively.

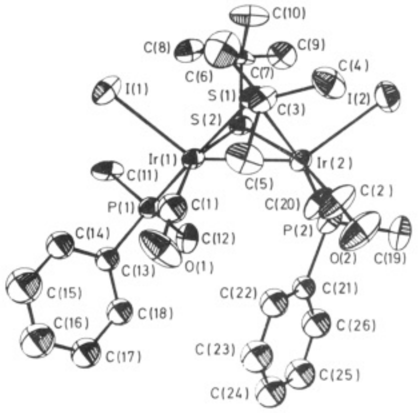

Figure 1. Perspective representation of the molecule **7**. The vibrational ellipsoids are drawn at 50% probability level. The labeling is also shown.

Table V. Bond Lengths (Å) for Compound 7

Ir(1)–Ir(2)	2.702 (1)	C(3)–C(5)	1.52 (3)
Ir(1)–I(1)	2.742 (2)	C(3)–C(6)	1.52 (3)
Ir(2)–I(2)	2.712 (2)	C(7)–C(8)	1.57 (3)
Ir(1)–P(1)	2.318 (5)	C(7)–C(9)	1.56 (3)
Ir(2)–P(2)	2.311 (5)	C(7)–C(10)	1.52 (3)
Ir(1)–S(1)	2.383 (5)	P(1)–C(11)	1.83 (2)
Ir(2)–S(1)	2.372 (5)	P(1)–C(12)	1.82 (2)
Ir(1)–S(2)	2.373 (5)	P(1)–C(13)	1.81 (2)
Ir(2)–S(2)	2.391 (5)	P(2)–C(19)	1.84 (2)
Ir(1)–C(1)	1.78 (3)	P(2)–C(20)	1.79 (2)
Ir(2)–C(2)	1.88 (2)	P(2)–C(21)	1.85 (2)
S(1)–C(3)	1.86 (2)	C(1)–O(1)	1.22 (3)
S(2)–C(7)	1.89 (2)	C(2)–O(2)	1.11 (2)
C(3)–C(4)	1.54 (3)		

Chlorine is the more powerful oxidative halide. Indeed, even in very dilute solutions of starting Ir(I) complexes, very fast changes of color are observed. The final products exhibit the +III oxidative state for iridium. Moreover, the thiolato bridges are replaced by chlorine atoms, the general reaction being as shown in eq 3 (L = CO, **14**; L = P(OMe)$_3$, **15**).

$$Ir_2(\mu\text{-}t\text{-}BuS)_2(CO)_2L_2 + Cl_2 \xrightarrow[\text{excess}]{} Ir_2(\mu\text{-}Cl)_2CO_2L_2Cl_4 \quad (3)$$

Description of the Structure of 7. The crystal structure involves the packing of four discrete dinuclear molecules per unit cell. Figure 1 shows a perspective view of molecule **7** along with the labeling scheme. Bond distances and angles of interest are given in Tables V and VI.

The overall structure can be described as two square-planar pyramids sharing an edge. It has roughly a mirror

---

(17) See paragraph at end of paper regarding supplementary material.

Table VI. Bond Angles (Deg) for Compound 7

I(1)-Ir(1)-S(1)	91.6 (1)	Ir(1)-S(1)-Ir(2)	69.3 (1)	S(2)-C(7)-C(9)	105.3 (13)
I(1)-Ir(1)-S(1)	107.5 (1)	Ir(1)-S(1)-C(3)	119.9 (6)	S(2)-C(7)-C(10)	114.5 (14)
I(1)-Ir(1)-P(1)	92.7 (1)	Ir(2)-S(1)-C(3)	118.5 (6)	C(8)-C(7)-C(9)	111.0 (16)
I(1)-Ir(1)-C(1)	94.9 (7)	Ir(1)-S(2)-Ir(2)	69.1 (1)	C(8)-C(7)-C(10)	109.5 (17)
I(2)-Ir(2)-S(1)	95.7 (1)	Ir(1)-S(2)-C(7)	124.4 (7)	C(9)-C(7)-C(10)	112.6 (16)
I(2)-Ir(2)-S(2)	102.0 (1)	Ir(2)-S(2)-C(7)	122.8 (6)	Ir(1)-P(1)-C(11)	114.6 (7)
I(2)-Ir(2)-P(2)	92.5 (1)	S(1)-C(3)-C(4)	106.5 (13)	Ir(1)-P(1)-C(12)	117.5 (7)
I(2)-Ir(2)-C(2)	92.0 (8)	S(1)-C(3)-C(5)	116.0 (13)	Ir(1)-P(1)-C(13)	126.0 (7)
P(1)-Ir(1)-S(1)	167.6 (2)	S(1)-C(3)-C(6)	102.8 (13)	Ir(2)-P(2)-C(19)	115.1 (8)
P(2)-Ir(2)-S(1)	170.2 (2)	C(4)-C(3)-C(5)	112.5 (17)	Ir(2)-P(2)-C(20)	116.3 (7)
P(1)-Ir(1)-S(2)	87.0 (2)	C(4)-C(3)-C(6)	109.8 (17)	Ir(2)-P(2)-C(21)	126.7 (7)
P(2)-Ir(2)-S(2)	92.5 (2)	C(5)-C(3)-C(6)	108.9 (18)	Ir(1)-C(1)-O(1)	173.1 (19)
P(1)-Ir(1)-C(1)	87.9 (6)	S(2)-C(7)-C(8)	103.6 (12)	Ir(2)-C(2)-O(2)	175.3 (22)
P(2)-Ir(2)-C(2)	88.0 (7)				

plane containing this edge. Indeed, each iridium atom is surrounded by five atoms, four of them being in a plane, i.e., S(1), S(2), C(1), and P(1) around Ir(1) and S(1), S(2), C(2), and P(2) around Ir(2). The fifth vertice of each pyramid is occupied by an iodine atom. Bond angles in Table VI clearly indicate a square-planar pyramidal type of environment around each iridium atom. The thiolato groups bridge the two iridium atoms, and the flap angle is 83.8°. The Ir(1)–Ir(2) distance of 2.702 (1) Å, together with the diamagnetism of the compound, strongly suggests an iridium–iridium bond. This bond distance has exactly the same value as the one observed in $(\mu\text{-CO})(\mu\text{-}t\text{-BuS})\text{Ir}_2(\text{S-}t\text{-BuS})(\text{CO})_2(\text{PMe}_3)_3$[10] an other dinuclear Ir(II) complex exhibiting a two-electron Ir–Ir single bond with two different bridges. It compares well with the value 2.673 (1) Å observed in $(\text{Ir(H)}(\mu\text{-t-BuS})(\text{CO})(\text{P(OMe)}_3)_2$[9] and $\text{Ir}_2(\text{C}_{10}\text{H}_4\text{S}_4)(\text{CO})_2(\text{PPh}_3)_2\text{Br}_2$,[18] a dinuclear Ir(II) complex with two thiolato-bridging groups as in the present compound. The Ir_2S_2 core shows an asymmetric bridging situation with two different Ir–S bond distances: Ir(I)–S(2) = 2.373 (5) Å and Ir(2)–S(1) = 2.372 (5) Å, on the one hand, and Ir(1)–S(1) = 2.383 (5) and Ir(2)–S(2) = 2.391 (5) Å on the other hand. This situation cannot be explained in terms of a trans influence. Indeed, the two phosphine ligands and the two carbonyl groups are mutually *cis*. The Ir–I bond distances observed in the present compound of 2.742 (2) and 2.712 (2) Å can be compared to the Rh–I bond distance of 2.761 (1) Å which is trans to a Rh–Rh bond in $((\text{PhCH}_2\text{NC})_{12}\text{Rh}_3\text{I}_3)^{3+}$[19] or the Ir–I bond distances which range from 2.68 to 2.75 Å in $\{\text{Ir}_2(\mu\text{-I})_3\text{I}_2(\text{PMePh}_2)_4\}^+$.[20] If we regard S(1) and S(2) as approximately tetrahedrally coordinated with the lone pair as the fourth virtual ligand, there the lone pair on S(1) is localized outside the dihedral angle in an exo position, while that one of S(2) is localized inside in an endo position. In other words, it can be said that the thiolato groups are in anti positions.[13]

The Ir_2S_2 core found in the present compound is more compact than the one observed in $\text{Ir}_2(\mu\text{-}t\text{-BuS})_2(\text{CO})_2\{\text{P(OMe)}_3\}_2$,[9] one of the starting complexes. Indeed, the Ir–Ir separation is 2.702 (1) Å instead of 3.216 (2) Å; the dihedral angle is 83.8° instead of 123.2°. This considerable compression of the four-membered Ir_2S_2 ring along the Ir–Ir axis is the major consequence of the oxidative addition of iodine on complexes **1**–**4**. It is worth noting that this addition does not affect the overall geometry of the starting complexes **1**–**4** since both dinuclear compounds exhibit a mutually cis arrangement about the phosphine (or phosphite) ligands.

The iridium–iodine bond lengths Ir(1)–I(1) = 2.742 (2) Å and Ir(2)–I(2) = 2.702 (1) Å are significantly different. We do not have at the present time any satisfactory reason to explain such a difference. Having in mind that two three-electron donor thiolato groups bridge the iridium atoms, one could make the hypothesis that the present compound is formed from different iridium atoms, one being an electron-rich metal center and the other one an electron-deficient metal center: a heteropolar homonuclear metal–metal bonding then could be invoked to explain the short Ir(1)–Ir(2) distance of 2.702 (1) Å as for instance for $\text{Ir}_2(\mu\text{-}t\text{-BuS})_2(\text{CO})_2(\text{P(OMe)}_3)_2(\text{C(CN)}_2)_2$.[21] Owing to the fact that the two ν_{CO} stretching frequencies are observed with too close values, i.e., 2007 and 1990 cm^{-1} and to the fact that the ^{31}P NMR spectrum of the parent complex $\text{Ir}_2(\mu\text{-}t\text{-BuS})_2(\text{CO})_2(\text{PMe}_3)_2\text{I}_2$ shows equivalent phosporus atoms, such an hypothesis cannot longer be pointed out.

Discussion. In complexes $\text{Ir}_2(\mu\text{-}t\text{-BuS})_2(\text{CO})_2\text{L}_2\text{I}_2$ (**5**–**8**) the iodine atoms occupy the apical positions as revealed by the X-ray structure of complex **7**. Two isomers have been found for $\text{Ir}_2(\mu\text{-}t\text{-BuS})_2(\text{CO})_4\text{I}_2$. For each isomer three CO stretching bands were observed in the infrared spectra, the relative intensities being similar to those found for the complexes $\text{Fe}_2(\mu\text{-SMe})_2(\text{CO})_4(\text{PR}_3)_2$[22] where the two phosphine ligands are in the apical positions. The isomerism is due to the different relative positions of the *tert*-butyl groups: two syn (exo and endo) ones having a C_{2v} symmetry and one anti isomer are expected. However, it has been previously shown for similar complexes[23] that, although the anti isomerism breaks down the C_{2v} symmetry to C_s, the vibrations of the coordinated carbonyl groups apparently obey the selection rules for the C_{2v} point group. We did not succeed in separating the two isomers by fractional crystallization or by chromatography, and the same mixture of isomers is observed at any reaction temperature with or without UV irradiation. The most abundant isomer is expected to be the syn-endo one. Indeed the ^{13}C NMR spectra of the starting $\text{Ir}_2(\mu\text{-}t\text{-BuS})_2(\text{CO})_4$ material with a syn-endo conformation[24] exhibits resonances at 49.27 ppm for the quaternary C atoms of the *t*-Bu groups and 33.94 ppm for the methyl groups, all values which agree well with those, 54.24, and 33.78 ppm, respectively, observed for the syn-endo isomer **5**. The second isomer is anti since the ^{1}H and ^{31}P spectra clearly reveal the presence of two magnetically nonequivalent *t*-Bu groups. The ^{13}C NMR spectrum confirms this type of

---

(18) Teo, B. K.; Snyder-Robinson, P. A. *J. Chem. Soc., Chem. Commun.* **1979**, 255.

(19) Balch, A. L.; Olmstead, M. L. *J. Am. Chem. Soc.* **1979**, *101*, 3128.

(20) Nolte, M. J.; Van Der Stok, E.; Singleton, E. *Inorg. Chim. Acta* **1976**, *19*, L51.

(21) Maisonnat, A.; Bonnet, J.-J.; Poilblanc, R. *Inorg. Chem.* **1980**, *19*, 3168.

(22) De Beer, J. A.; Haines, R. J.; Greatex, R.; Greenwood, N. N. *J. Chem. Soc. A* **1971**, 3271.

(23) Palvi, G.; Vizi-Orosz, A.; Marko, L.; Marcati, F.; Bor, G. *J. Organomet. Chem.* **1974**, *66*, 295.

(24) Bonnet, J.-J.; Galy, J.; de Montauzon, D.; Poilblanc, R. *J. Chem. Soc., Chem. Comm.* **1977**, 47.

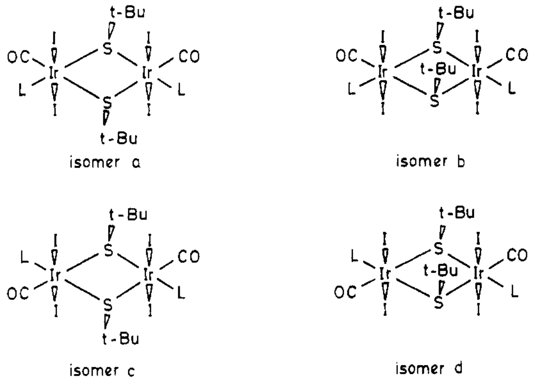

isomer a

isomer b

isomer c

isomer d

Figure 2. Various isomers expected for complexes $Ir_2(\mu\text{-}t\text{-}BuS)(CO)_2L_2I_4$.

isomer, the resonances at 52.23 and 33.78 ppm corresponding, respectively, to the CS and CH_3 in the endo position, whereas those at 60.76 and 34.78 ppm correspond to the exo *t*-Bu group.

For complex **7** (L = PMe_2Ph) the ^1H NMR spectrum proves that only one isomer is obtained. The X-ray structure shows a cis-anti conformation. Due to its low solubility in CD_2Cl_2, no ^{13}C NMR data are available. In the case of complex **6** (L = $P(OMe)_3$) only one isomer is observed, and ^{31}P, ^1H, and ^{13}C NMR spectra indicate a cis-anti conformation as for complex **7**. When L = PMe_3, complex **8** is observed as a mixture of two isomers which were easily separated by fractional crystallization. ^{31}P, ^1H, and ^{13}C NMR data are consistent with a cis-anti conformation for the first isomer as for previous complexes **6** and **7**. For the second isomer **8**, the ^{31}P data show the two phosphorus atoms to be magnetically nonequivalent. Moreover the ^{13}C NMR signals at 52.99 and 57.55 ppm for the quaternary C atoms of the *t*-Bu groups suggest a trans-anti conformation.

About the mechanism of addition of iodine, several routes can be ruled out. One can first imagine an ionic process with a stepwise electrophilic attack of I^+ at the first metal center followed by a nucleophilic attack of I^- on the second metal center. We do not favor this process. Indeed, addition of iodine in the presence of an excess of KBr dissolved in acetone failed to give a complex in which I and Br would appear together. Then, an ionic process with a nucleophilic attack of I^- in the first step also is rejected since no reaction has been observed with the starting $Ir_2(\mu\text{-}t\text{-}BuS)_2CO_2L_2$ materials in the presence of large excess of NaI.

Although attempts to observe EPR signals during iodine or CH_3I addition in the presence of a nitrone spin trap failed to reveal radical intermediates, we favor a radical process from the following observation. Addition of glavinoxyl to $Ir_2(\mu\text{-}t\text{-}BuS)_2CO_2L_2$ gives an intense red-violet color. Further addition of some drops of a dilute solution of iodine in the absence of natural light induces a decoloration of the solution which can be interpreted as a capture of an iodine radical by the galvinoxyl. The solution takes then the red color of the expected complexes $Ir_2(\mu\text{-}t\text{-}BuS)_2(CO)_2L_2I_2$. We observed a very fast oxidative addition of iodine which occurs even at low temperatures (down to −20 °C).

With regard to the tetraiodo or tetrabromo complexes of type $Ir_2(\mu\text{-}t\text{-}BuS)_2(CO)_2L_2X_4$, no attempt to separate the various isomers obtained through either further addition of 1 mol of iodine to $Ir_2(\mu\text{-}t\text{-}BuS)_2(CO)_2L_2I_2$ complexes or addition of 2 mol of bromine to $Ir_2(\mu\text{-}t\text{-}BuS)_2(CO)_2L_2$ has been carried out.

Infrared spectra do not account for the presence of various isomers. Indeed, the ν_{CO} stretching bands are in any case broad. If one assumes that the two extra halogens enter in the apical positions, as the previous one in $Ir_2(\mu\text{-}t\text{-}BuS)_2(CO)_2L_2I_2$, the ^1H NMR spectra are quite useful to account for the various isomers: first it can be said that in all cases the signals of the *t*-Bu groups are within the range for such groups in bridging positions, result being considered with the hypothesis of four various isomers (Figure 2) if L is not CO. Indeed, such complexes have a planar Ir_2S_2 core as referred to the parent dinuclear $\{RhClBr(CH_3)(CO)PMe_2Ph\}_2$ whose X-ray structure has been determined.[25] when L = CO, two isomers are observed. This result is the expected one since two diiodo complexes, the syn and anti isomers, were detected.

When L = $P(OMe_3)_3$, an unexpected result is observed since four isomers are detected. Indeed, these isomers are obtained starting with a simple cis-anti diiodo complex and thus one could expect to observe only the isomer a. No attempt to determine the rearrangement process has been carried out.

In the case of the chlorine addition, this isomerization proceeds further and gives rise to substitution of the *t*-BuS-bridging group by chlorine atoms.

Registry No. 1, 63312-27-6; 2, 63292-76-2; 3, 74183-89-4; 4, 63292-79-5; *anti*-**5**, 74144-12-0; *syn-endo*-**5**, 74183-90-7; **6**, 74144-13-1; **7**, 74144-14-2; *cis-anti*-**8**, 74144-15-3; *trans-anti*-**8**, 74183-91-8; **9**, 82246-63-7; **10**, 82246-64-8; **11**, 82264-82-2; **12**, 82246-65-9; **13**, 82246-66-0; **14**, 82246-67-1; **15**, 82264-83-3.

Supplementary Material Available: Table I, crystal data, Table IV, root-mean-square amplitudes, and a listing of structure factor amplitudes (19 pages). Ordering information is given on any current masthead page.

---

[25] Doyle, M. J.; Mayanza, A.; Bonnet, J.-J.; Kalck, Ph.; Poilblanc, R. *J. Organomet. Chem.* **1978**, *146*, 293.